Letter

Anomalous transport in the kinetically constrained quantum East-West model

Pietro Brighi [1] and Marko Ljubotina [2]

[1]*Faculty of Physics, University of Vienna, Boltzmanngasse 5, 1090 Vienna, Austria*
[2]*Institute of Science and Technology Austria (ISTA), Am Campus 1, 3400 Klosterneuburg, Austria*

We study a chaotic particle-conserving kinetically constrained model, with a single parameter which allows us to break reflection symmetry. Through extensive numerical simulations we find that the domain wall state shows a variety of dynamical behaviors from localization all the way to ballistic transport, depending on the value of the reflection breaking parameter. Surprisingly, such anomalous behavior is not mirrored in infinite-temperature dynamics, which appear to scale diffusively, in line with expectations for generic interacting models. However, studying the particle density gradient, we show that the lack of reflection symmetry affects infinite-temperature dynamics, resulting in an asymmetric dynamical structure factor. This is in disagreement with normal diffusion and suggests that the model may also exhibit anomalous dynamics at infinite temperature in the thermodynamic limit. Finally, we observe low-entangled eigenstates in the spectrum of the model, a telltale sign of quantum many-body scars.

Introduction. Out-of-equilibrium properties of many-body systems present one of the central problems in quantum statistical mechanics. Of particular interest are the different universality classes of dynamics found in various models. Typically, generic chaotic models are expected to behave diffusively [1–10], although slower dynamics were observed in disordered systems [4,11–16].

Recently, however, it was shown that certain chaotic kinetically constrained models (KCMs) can exhibit superdiffusive dynamics at infinite temperature [17]. Such nondiffusive behavior was observed both in particle [18] and energy transport [17]. Additionally, anomalous dynamics can also arise at the level of pure states [19–24], as in the celebrated PXP model, where certain states show long-lived oscillations in the density of domain walls [21,25].

Besides anomalous dynamical features, kinetically constrained models, first introduced in the context of classical glasses [26–28], also host other remarkable phenomena. These range from Hilbert space fragmentation [29–35] to quantum many-body scars [21,36–45], defining the novel paradigm of weak ergodicity breaking [46].

A paradigamtic example of KCMs is the celebrated quantum East model [19]. The quantum East model hosts a localization transition in the ground state [22,47] and extremely slow dynamics [19,47], while its Floquet version has shown localized behavior [48] as well as an exactly solvable point in parameter space [49]. However, the model only has a single conserved charge, the energy, which itself is not present in the Floquet version.

A recent work [24] introduced a particle-conserving version of the quantum East model. The combination of $U(1)$ symmetry and kinetic constraints leads to classical and quantum Hilbert space fragmentation, i.e., fragmentation in an entangled basis [35], and to a dramatic effect on dynamics, which show superdiffusive behavior in certain initial states [24].

In this Letter we explore the interplay between reflection symmetry and kinetic constraints. Specifically, we focus on the dynamics of a constrained hopping model, inspired by the particle-conserving quantum East model [24]. In the original model hopping is allowed between two neighboring sites if the site immediately to the right of the pair is occupied. Here, we add the reflection-symmetric *West* constrained hopping term, with a potentially different amplitude. This also allows particle hopping when the nearest neighbor on the left is occupied, regardless of the state of the right neighbor. The addition of this term breaks both classical and quantum fragmentation, allowing us to study infinite-temperature transport in the dominant fragment of the Hilbert space and control the reflection symmetry.

In spite of the absence of fragmentation and chaotic level spacing statistics, the spectrum of the Hamiltonian still presents intriguing characteristics [50]. In particular, we find a large number of zero modes which depends on particle parity and a set of weakly entangled eigenstates reminiscent of quantum many-body scars [21,36].

Studying the dynamics of the domain wall state [51,52], a simple and experimentally accessible initial state, we discover the presence of a rich phase diagram dependent on the ratio of the two hopping terms. In our simulations we observe a full spectrum of different dynamical behaviors of the domain wall state ranging from completely localized to a surprising ballistic behavior, in spite of the chaotic nature of the model. This suggests that ballistic transport, typically observed in integrable models, which has been related to superconductivity [53,54], can also be observed in the dynamics of pure states of certain generic chaotic models. Upon increasing the West hopping term beyond the symmetric point, where the two hopping amplitudes are equal, the state recovers the expected diffusive spreading. However, when the East constraint is completely suppressed, we again observe anomalous dynamics, this time with superdiffusive scaling up to the available times.
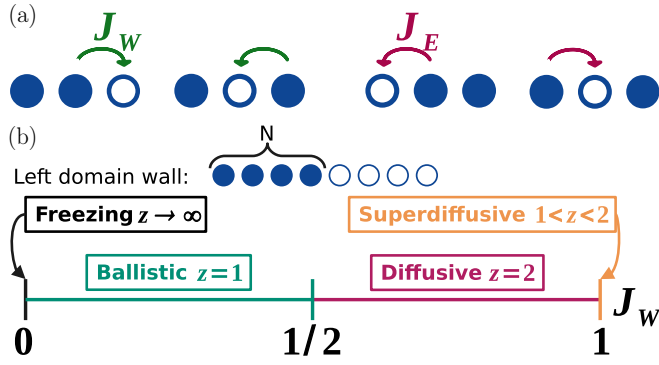
FIG. 1. (a) Particles move with different hopping amplitudes $J_E = 1 - J_W$ depending on whether the constraint is applied from the left or the right neighbor. (b) As J_W is changed from 0 to 1, the dynamical behavior of the *left domain wall* (LDW) state, shown here for the small case of $N = 4$ particles and $L = 8$ sites, changes dramatically. Its dynamics show a transition from fully localized at $J_W = 0$ to ballistic for $J_W \leqslant 1/2$ and to the expected diffusive behavior as J_W is increased further. However, at the opposite extreme ($J_W = 1$) the dynamics appear to enter an anomalous superdiffusive regime. Here, the dynamical exponent z corresponds to that from Eq. (3), computed only from the LDW state.

Using tensor-network methods, we further probe infinite-temperature dynamics which indicate diffusive scaling. However, analyzing the dynamical structure factor at infinite temperature [55], we observe long-lived asymmetry. This finite asymmetry is at odds with normal diffusion and shows another intriguing anomaly of transport in this model.

Model. We study kinetically constrained hard-core bosons on a one-dimensional lattice of L sites. Hopping among different sites is allowed only in certain configurations, as encoded in the system Hamiltonian

$$\hat{H} = J_W \sum_{i=1}^{L-2} \hat{n}_i (\hat{c}_{i+2}^\dagger \hat{c}_{i+1} + \text{H.c.})$$
$$+ J_E \sum_{i=1}^{L-2} (\hat{c}_{i+1}^\dagger \hat{c}_i + \text{H.c.}) \hat{n}_{i+2} = J_E \hat{H}_E + J_W \hat{H}_W, \quad (1)$$

where $\hat{H}_E$ ($\hat{H}_W$) is the $U(1)$-conserving East (West) Hamiltonian, $\hat{c}_i^\dagger$ is the hard-core boson creation operator, and $\hat{n}_i = \hat{c}_i^\dagger \hat{c}_i$ is the particle number operator. The action of the two kinetic constraints is sketched in Fig. 1(a). Particles can hop only if their nearest neighbor *to the left* (West) or *to the right* (East) is occupied, with amplitudes J_W and J_E, respectively. Throughout this Letter, we fix the two hopping parameters such that $J_E + J_W = 1$. As we will show in the following, varying the parameter J_W leads to the dramatic change in dynamics of the domain wall state [51,52] depicted in Fig. 1(b).

Besides being particle conserving, the Hamiltonian (1), with periodic boundary conditions, is also translation invariant. At the *symmetric point* $J_E = J_W = 1/2$ the system is further reflection symmetric. As opposed to the closely related quantum East model, no additional symmetry emerges and the system does not exhibit Hilbert space fragmentation away from $J_W \in \{0, 1\}$, at least within the half-filling sector on which we focus in this Letter. Despite the absence of

Hilbert space fragmentation, the analysis of the spectrum and of the eigenstates of the Hamiltonian yields interesting observations [50]. On one hand the study of the level spacing distribution confirms that the system is overall chaotic. On the other, we notice the presence of a small number of weakly entangled eigenstates, reminiscent of quantum many-body scars. Finally, the spectrum presents an anomalously large number of zero modes, which appear only for *even* particle numbers $N = L/2$.

Domain wall dynamics. We now focus on the dynamics after a quantum quench in our system with open boundary conditions. Our protocol consists of initializing the system in the left domain wall state,

$$|\text{LDW}\rangle = |\underbrace{\bullet \bullet \bullet \cdots \bullet}_{N} \underbrace{\circ \circ \circ \cdots \circ}_{L-N}\rangle \quad \begin{array}{l} \hat{n}_i|\bullet\rangle = |\bullet\rangle, \\ \hat{n}_i|\circ\rangle = 0, \end{array} \quad (2)$$

which at $J_W = 0$ is an exact zero-energy eigenstate of the Hamiltonian. We then suddenly switch the West hopping amplitude to its final value $J_W \in (0, 1]$.

To study the dynamics of $|\text{LDW}\rangle$ we perform numerical simulations over an extensive number of system sizes $L \in [14, 100]$, using exact techniques for $L \leqslant 24$ and approximate matrix-product-state time evolution using the time-evolving block-decimation (TEBD) algorithm [56] for $L > 24$ [50]. Our analysis focuses on the instantaneous dynamical exponent $z(t)$ defining the dynamical behavior of the state [57]. For interacting chaotic systems such as the one we study, particle spreading in generic high-temperature ensembles is expected to be diffusive ($z = 2$). Deviations from this behavior are known in integrable models [58], which can present ballistic ($z = 1$) and superdiffusive ($1 < z < 2$) transport [9,10,55,59–62], and in disordered systems with subdiffusive dynamics ($z > 2$) [4,12]. Here, instead, we focus on a single pure state, similarly to previous studies of the domain wall state in the XXZ chain [51,52], with weight over the entire spectrum. To numerically obtain the instantaneous dynamical exponent, we take the logarithmic derivative of the particle flow from the domain wall,

$$\delta N(t) = \sum_{i=1}^{N} \langle \hat{n}_i(t = 0)\rangle - \langle \hat{n}_i(t)\rangle, \quad \delta N(t) \propto t^{1/z}, \quad (3)$$

$$\frac{1}{z} = \frac{d \log \delta N}{d \log t}. \quad (4)$$

In Fig. 2 we show the particle dynamics of the domain wall quench [Figs. 2(a)–2(d)] as well as the instantaneous dynamical exponent [Figs. 2(e)–2(h)] at different values of J_W, highlighting the variety of different behaviors in our model. When $J_W < 1/2$ the dynamics of $|\text{LDW}\rangle$ initially are, as expected, relatively slow due to the combination of dominant East constraint and large particle density in the left half [Fig. 2(a)]. Surprisingly, however, the transport exponent shows clear ballistic scaling $z = 1$ [Fig. 2(e)]. This behavior persists up to times proportional to the system size due to finite-size effects. A similar behavior, although with much faster particle spreading, is observed for $J_W = 1/2$, shown in Figs. 2(b) and 2(f). In both cases the results indicate ballistic dynamics of $|\text{LDW}\rangle$ in the thermodynamic limit.

As the hopping amplitude is increased even further, entering the regime where $J_W > J_E$, the domain wall recovers
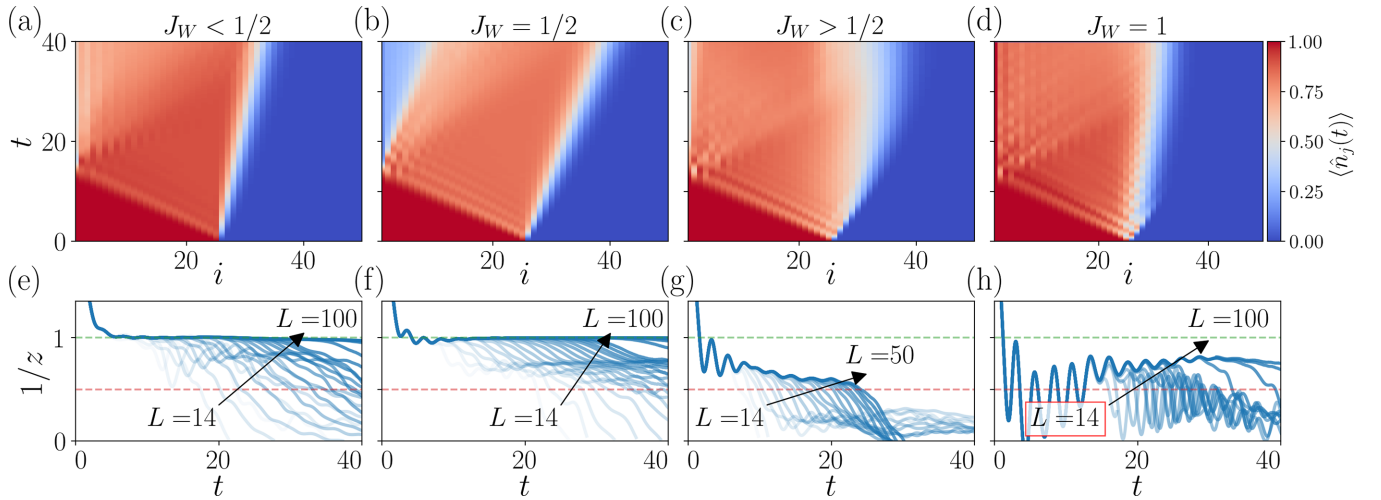
FIG. 2. Density dynamics of |LDW⟩ dramatically changes as J_W is tuned across the symmetric point $J_W = 1/2$ [(a)–(d)]. While the model is fully chaotic and its infinite-temperature dynamics appear to scale diffusively, for $J_W \leqslant 1/2$, |LDW⟩ shows ballistic behavior [(a), (b)]. However, as $J_W > 1/2$ (c), (d)], the |LDW⟩ state deviates from the ballistic regime. This clearly emerges looking at the instantaneous dynamical exponent $z(t)$, whose inverse is shown in (e)–(h). For $J_W \leqslant 1/2$ [(e), (f)] the dynamical exponent presents a long plateau at $z^{-1} = 1$ corresponding to ballistic behavior. This eventually changes when finite-size effects are observed at a critical time $\tau \propto L$. Therefore we extract z from times where the largest two system sizes have not yet diverged in order to avoid the finite-size effects. For $1/2 < J_W < 1$ (g), the inverse dynamical exponent quickly decays below 1, relaxing at long times to a value close to diffusion $z^{-1} = 1/2$. Finally, as the East contribution vanishes, $J_W = 1$ (h), |LDW⟩ acquires an unexpected superdiffusive behavior, with the dynamical exponent rapidly oscillating at first, and later approaching a value well above diffusion. The dashed lines in the bottom row correspond to diffusive and ballistic behavior (red and green, respectively). The data were generated for $J_W = 1/3, 1/2, 2/3, 1$ using exact methods for $L \leqslant 24$ and TEBD with bond dimension $\chi = [1536, 2048]$ for $L \geqslant 26$.

the expected diffusive behavior, as shown by the dynamical exponent $1/z \to 1/2$ in Fig. 2(g). However, at the extreme point $J_W = 1$, where only the West Hamiltonian participates in the dynamics, the domain wall state acquires yet another unexpected dynamical exponent. As shown in Fig. 2(h), after a series of initial oscillations damping with systems size, $1/z$ approaches a superdiffusive value, which at the timescales attainable by our simulations is approximately $1/z \approx 0.8$.

While superdiffusion in the particle-conserving East model was recently observed [24] with exact diagonalization, here we discover that introducing the additional West constraint and tuning the asymmetry between the two yields the rich dynamical *phase diagram* for the domain wall state shown in Fig. 1(b). In particular, the presence of a ballistic state in an otherwise chaotic model is highly atypical [63]. Finally, we mention that for $J_W \ll J_E$ we notice a striking difference in dynamics depending on the particle number N (akin to the number of zero modes discussed previously). For even N, particles are confined within a small region and cannot explore the full lattice, while for odd N they spread ballistically through the whole chain [50].

Persistent asymmetry at infinite temperature. To further characterize the dynamics in the model, we analyze the dynamical exponent of mixed states close to infinite temperature $\rho_0 = \otimes_i \rho_0^{(i)}$,

$$\rho_0^{(i)} = \begin{pmatrix} 1/2 + \mu(i) & 0 \\ 0 & 1/2 - \mu(i) \end{pmatrix},$$

$$\mu(i) = \begin{cases} \mu_0, & i \leqslant L/2, \\ -\mu_0, & i > L/2, \end{cases} \tag{5}$$

with $\mu_0 \ll 1$ [61]. Using TEBD, we simulate the dynamics of a system of $L = 512$ sites in a wide parameter range $J_W \in [0.15, 0.5]$ and $\mu \in [0.001, 0.1]$.

First, we focus on the dynamical exponent z. To get an estimate of its value, we perform a collapse of the density profiles at different times, shown in Fig. 3. Given the dynamical exponent, density dynamics are expected to be captured by a scale-invariant function $f(x/t^{1/z})$. The different curves in Fig. 3 collapse on one another within a broad range of times as the space axis is rescaled by $\sqrt{t}$, suggesting diffusive scaling. This observation is further confirmed by the dynamical exponent approaching $z = 2$ at late times, as reported in the inset. Similar results are obtained for other values of the hopping parameters [50]. The usual diffusive behavior, then, seems to
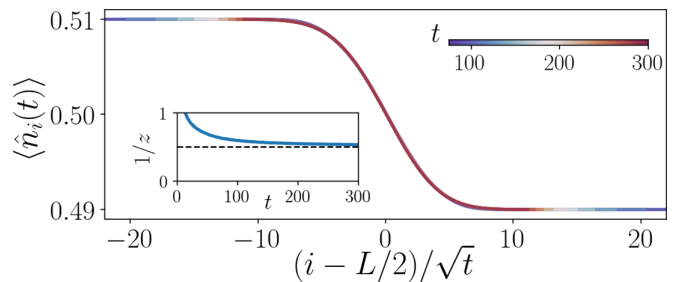
FIG. 3. Mixed state density profiles at different times $t \in [75, 300]$ collapse on one another upon rescaling the x axis by $\sqrt{t}$ suggesting diffusive scaling at infinite temperature. The diffusive scaling is further confirmed by the dynamical exponent approaching $z^{-1} \approx 0.5$ at late times, as shown in the inset. The data shown here are for $J_W = 1/2$, $\mu = 0.01$, and $\chi = 384$.
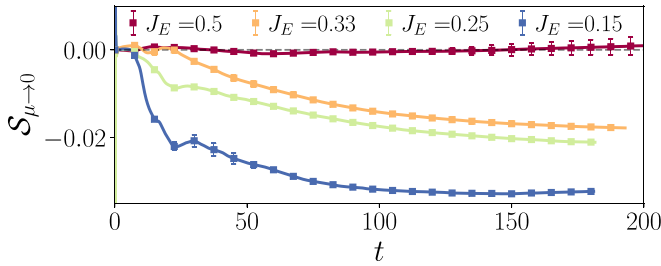
FIG. 4. The extrapolation of the skewness $\mathcal{S}$ for $\mu \to 0$ shows a finite long-time value for $J_W < 1/2$, indicating persistent asymmetry even in the absence of the initial chemical potential step. The late time behavior of the skewness as a function of J_W shows a monotonic decrease of the asymmetry as $J_W \to 0$. Due to reflection symmetry, a mirrored behavior appears with positive $\mathcal{S}$ at $J_W > 1/2$. The data were obtained by extrapolating the intercept of a linear fit of $\mathcal{S}(t)$ vs μ for values of $\mu \in [0.001, 0.05]$. The system size is $L = 512$ sites, and the bond dimension used was $\chi = 448$.

be recovered at high temperature. We note that tiny but nonvanishing faster-than-diffusive corrections would be difficult to identify and thus cannot be ruled out. Therefore, there could be other states that share the same ballistic behavior as the $|\text{LDW}\rangle$ state, so long as they remain a sufficiently small or vanishing fraction of the Hilbert space size.

In a diffusive system, particle spreading is expected to be symmetric around the central chemical potential step μ. Our model, however, is inherently *asymmetric* and could deviate from this behavior. To characterize this possible asymmetry, we analyze the particle density gradient $\Delta n_{i,i+1} = |\langle \hat{n}_i \rangle_\mu - \langle \hat{n}_{i+1} \rangle_\mu|$, which is related to the dynamical structure factor $S(x, t) = \langle \hat{n}_x(t) \hat{n}_0(0) \rangle = \lim_{\mu \to 0} \frac{1}{\mu} \Delta n_{x,x+1}$ [55]. Here, $\langle \hat{O} \rangle_\mu$ represents the expectation value of the operator with the weak domain wall initial state from Eq. (5).

The asymmetric constraints in our Hamiltonian together with the asymmetric initial state, instead, yield rather a *skewed* distribution (see Supplemental Material [50] for some examples). To quantitatively capture the amount of asymmetry in the state at a given time, we calculate the discrete skewness of the dynamical structure factor,

$$\mathcal{S} = \sum_y \mathcal{P}_{\Delta n}(y) \left(\frac{y - \mu_1}{\sigma} \right)^3. \qquad (6)$$

Here, $\mathcal{P}_{\Delta n}$ is the normalized particle density gradient, and μ_1 and σ are the corresponding mean and standard deviation.

For all finite μ, the skewness relaxes to a finite negative value at long times. As we take the linear response limit $\mu \to 0$ and the asymmetry of the initial state vanishes, however, $\mathcal{S}$ is expected to vanish proportionally following the expectations for normal diffusion. Using a linear fit, we extrapolate the skewness at $\mu = 0$ [50], which we show in Fig. 4.

Surprisingly, whenever $J_W \neq J_E$ a finite skewness persists at $\mu = 0$. At the symmetric point, instead, skewness vanishes, as expected due to the symmetries in that case. Comparing $\mathcal{S}_{\mu \to 0}$ at late times we observe a monotonic increase of the skewness as a function of J_W, crossing zero at the symmetric point.

While this may be expected for an asymmetric model, the *asymmetric diffusive behavior* we observe deviates from

expectations for diffusion. This suggests that, while the bare transport exponent is not affected by the kinetic constraint, dynamics in general are, revealing a novel anomalous dynamical feature caused by the interplay of kinetic constraints and a lack of reflection symmetry.

Conclusions. In this Letter we studied the influence of kinetic constraints in combination with breaking reflection symmetry on the dynamical properties of quantum many-body systems. Specifically, we generalized the particle-conserving quantum East model [24] allowing also for West constrained hopping. While the system exhibits chaotic level spacing statistics, we find a pure state with anomalous dynamics. Within a range of the model parameter J_W, the dynamics from the LDW state exhibit several different types of transport ranging from the more typical insulating and diffusive dynamics to superdiffusion and even ballistic dynamics, typically associated to integrable systems [64–66]. The discovery of anomalous dynamics in the LDW state invites further research into the model, specifically identifying other states sharing similar dynamics would be extremely insightful. Furthermore, the observation of ballistic dynamics in a generic state in a chaotic model invites further research into models with broken reflection symmetry in order to understand the underlying properties that give rise to such dynamics.

We further observed diffusive scaling at infinite temperature, consistent with the model's ergodic nature. However, the finite asymmetry we observed implies that the dynamics are not described by a diffusion equation with a constant diffusion coefficient. Indeed, due to the nature of the model, one might argue that the diffusion constant should depend on the particle density, which could explain our observations, however, the exact nature of this dependence remains an open question. Interestingly, the direction of the asymmetry suggests the existence of many states moving faster to the left, in contrast to the LDW state moving ballistically to the right. These discrepancies present interesting open questions for future research, which would allow us to improve our understanding on the effects of breaking reflection symmetry on the dynamical properties of many-body quantum systems.

Moving from dynamical to spectral properties, we observe certain anomalies in the spectrum. Prominently, our model hosts a set of weakly entangled eigenstates, reminiscent of quantum many-body scars [21,36], and an anomalously large number of zero modes only for *even* particle number. Here, similarly to the PXP model, these weakly entangled eigenstates are not engineered [67], hence the model represents a potential avenue to improve our understanding of scars in other similar models.

[1] T. Prosen and M. Žnidarič, Diffusive high-temperature transport in the one-dimensional Hubbard model, Phys. Rev. B **86**, 125118 (2012).

[2] C. Karrasch, J. E. Moore, and F. Heidrich-Meisner, Real-time and real-space spin and energy dynamics in one-dimensional spin-$\frac{1}{2}$ systems induced by local quantum quenches at finite temperatures, Phys. Rev. B **89**, 075139 (2014).

[3] J. Lux, J. Müller, A. Mitra, and A. Rosch, Hydrodynamic long-time tails after a quantum quench, Phys. Rev. A **89**, 053608 (2014).

[4] M. Žnidarič, A. Scardicchio, and V. K. Varma, Diffusive and subdiffusive spin transport in the ergodic phase of a many-body localizable system, Phys. Rev. Lett. **117**, 040601 (2016).

[5] Y. Gu, X.-L. Qi, and D. Stanford, Local criticality, diffusion and chaos in generalized Sachdev-Ye-Kitaev models, J. High Energy Phys. 05 (2017) 125.

[6] M. Blake, R. A. Davison, and S. Sachdev, Thermal diffusivity and chaos in metals without quasiparticles, Phys. Rev. D **96**, 106008 (2017).

[7] A. J. Friedman, S. Gopalakrishnan, and R. Vasseur, Diffusive hydrodynamics from integrability breaking, Phys. Rev. B **101**, 180302(R) (2020).

[8] J. De Nardis, M. Medenjak, C. Karrasch, and E. Ilievski, Universality classes of spin transport in one-dimensional isotropic magnets: The onset of logarithmic anomalies, Phys. Rev. Lett. **124**, 210605 (2020).

[9] B. Bertini, F. Heidrich-Meisner, C. Karrasch, T. Prosen, R. Steinigeweg, and M. Žnidarič, Finite-temperature transport in one-dimensional quantum lattice models, Rev. Mod. Phys. **93**, 025003 (2021).

[10] D. Wei, A. Rubio-Abadal, B. Ye, F. Machado, J. Kemp, K. Srakaew, S. Hollerith, J. Rui, S. Gopalakrishnan, N. Y. Yao, I. Bloch, and J. Zeiher, Quantum gas microscopy of Kardar-Parisi-Zhang superdiffusion, Science **376**, 716 (2022).

[11] D. Basko, I. Aleiner, and B. Altshuler, Metal–insulator transition in a weakly interacting many-electron system with localized single-particle states, Ann. Phys. **321**, 1126 (2006).

[12] K. Agarwal, S. Gopalakrishnan, M. Knap, M. Müller, and E. Demler, Anomalous diffusion and Griffiths effects near the many-body localization transition, Phys. Rev. Lett. **114**, 160401 (2015).

[13] Y. Bar Lev, G. Cohen, and D. R. Reichman, Absence of diffusion in an interacting system of spinless fermions on a one-dimensional disordered lattice, Phys. Rev. Lett. **114**, 100601 (2015).

[14] J. Z. Imbrie, On many-body localization for quantum spin chains, J. Stat. Phys. **163**, 998 (2016).

[15] Y. Bar Lev, D. M. Kennes, C. Klöckner, D. R. Reichman, and C. Karrasch, Transport in quasiperiodic interacting systems: From superdiffusion to subdiffusion, Europhys. Lett. **119**, 37003 (2017).

[16] M. Žnidarič and M. Ljubotina, Interaction instability of localization in quasiperiodic systems, Proc. Natl. Acad. Sci. USA **115**, 4595 (2018).

[17] M. Ljubotina, J.-Y. Desaules, M. Serbyn, and Z. Papić, Superdiffusive energy transport in kinetically constrained models, Phys. Rev. X **13**, 011033 (2023).

[18] H. Singh, B. A. Ware, R. Vasseur, and A. J. Friedman, Subdiffusion and many-body quantum chaos with kinetic constraints, Phys. Rev. Lett. **127**, 230602 (2021).

[19] M. van Horssen, E. Levi, and J. P. Garrahan, Dynamics of many-body localization in a translation-invariant quantum glass model, Phys. Rev. B **92**, 100305(R) (2015).

[20] Z. Lan, M. van Horssen, S. Powell, and J. P. Garrahan, Quantum slow relaxation and metastability due to dynamical constraints, Phys. Rev. Lett. **121**, 040603 (2018).

[21] C. J. Turner, A. A. Michailidis, D. A. Abanin, M. Serbyn, and Z. Papić, Weak ergodicity breaking from quantum many-body scars, Nat. Phys. **14**, 745 (2018).

[22] N. Pancotti, G. Giudice, J. I. Cirac, J. P. Garrahan, and M. C. Bañuls, Quantum East model: Localization, nonthermal eigenstates, and slow dynamics, Phys. Rev. X **10**, 021051 (2020).

[23] R. J. Valencia-Tortora, N. Pancotti, and J. Marino, Kinetically constrained quantum dynamics in superconducting circuits, PRX Quantum **3**, 020346 (2022).

[24] P. Brighi, M. Ljubotina, and M. Serbyn, Hilbert space fragmentation and slow dynamics in particle-conserving quantum East models, SciPost Phys. **15**, 093 (2023).

[25] H. Bernien, S. Schwartz, A. Keesling, H. Levine, A. Omran, H. Pichler, S. Choi, A. S. Zibrov, M. Endres, M. Greiner, V. Vuletić, and M. D. Lukin, Probing many-body dynamics on a 51-atom quantum simulator, Nature (London) **551**, 579 (2017).

[26] G. H. Fredrickson and H. C. Andersen, Kinetic Ising model of the glass transition, Phys. Rev. Lett. **53**, 1244 (1984).

[27] W. Kob and H. C. Andersen, Kinetic lattice-gas model of cage effects in high-density liquids and a test of mode-coupling theory of the ideal-glass transition, Phys. Rev. E **48**, 4364 (1993).

[28] F. Ritort and P. Sollich, Glassy dynamics of kinetically constrained models, Adv. Phys. **52**, 219 (2003).

[29] T. Rakovszky, P. Sala, R. Verresen, M. Knap, and F. Pollmann, Statistical localization: From strong fragmentation to strong edge modes, Phys. Rev. B **101**, 125126 (2020).

[30] V. Khemani, M. Hermele, and R. Nandkishore, Localization from Hilbert space shattering: From theory to physical realizations, Phys. Rev. B **101**, 174204 (2020).

[31] Z.-C. Yang, F. Liu, A. V. Gorshkov, and T. Iadecola, Hilbert-space fragmentation from strict confinement, Phys. Rev. Lett. **124**, 207602 (2020).

[32] B. Pozsgay, T. Gombor, A. Hutsalyuk, Y. Jiang, L. Pristyák, and E. Vernier, Integrable spin chain with Hilbert space fragmentation and solvable real-time dynamics, Phys. Rev. E **104**, 044106 (2021).

[33] B. Mukherjee, D. Banerjee, K. Sengupta, and A. Sen, Minimal model for Hilbert space fragmentation with local constraints, Phys. Rev. B **104**, 155117 (2021).

[34] L. Zadnik and M. Fagotti, The folded spin-1/2 XXZ model: I. Diagonalisation, jamming, and ground state properties, SciPost Phys. Core **4**, 010 (2021).

[35] S. Moudgalya and O. I. Motrunich, Hilbert space fragmentation and commutant algebras, Phys. Rev. X **12**, 011050 (2022).

[36] C. J. Turner, A. A. Michailidis, D. A. Abanin, M. Serbyn, and Z. Papić, Quantum scarred eigenstates in a Rydberg atom chain: Entanglement, breakdown of thermalization, and stability to perturbations, Phys. Rev. B **98**, 155134 (2018).

[37] S. Moudgalya, N. Regnault, and B. A. Bernevig, Entanglement of exact excited states of Affleck-Kennedy-Lieb-Tasaki models: Exact results, many-body scars, and violation of the strong eigenstate thermalization hypothesis, Phys. Rev. B **98**, 235156 (2018).

[38] S. Choi, C. J. Turner, H. Pichler, W. W. Ho, A. A. Michailidis, Z. Papić, M. Serbyn, M. D. Lukin, and D. A. Abanin, Emergent SU(2) dynamics and perfect quantum many-body scars, Phys. Rev. Lett. **122**, 220603 (2019).

[39] T. Iadecola, M. Schecter, and S. Xu, Quantum many-body scars from magnon condensation, Phys. Rev. B **100**, 184312 (2019).

[40] W. W. Ho, S. Choi, H. Pichler, and M. D. Lukin, Periodic orbits, entanglement, and quantum many-body scars in constrained models: Matrix product state approach, Phys. Rev. Lett. **122**, 040603 (2019).

[41] A. Hudomal, I. Vasić, N. Regnault, and Z. Papić, Quantum scars of bosons with correlated hopping, Commun. Phys. **3**, 99 (2020).

[42] H. Zhao, J. Vovrosh, F. Mintert, and J. Knolle, Quantum many-body scars in optical lattices, Phys. Rev. Lett. **124**, 160604 (2020).

[43] H. Zhao, A. Smith, F. Mintert, and J. Knolle, Orthogonal quantum many-body scars, Phys. Rev. Lett. **127**, 150601 (2021).

[44] K. Tamura and H. Katsura, Quantum many-body scars of spinless fermions with density-assisted hopping in higher dimensions, Phys. Rev. B **106**, 144306 (2022).

[45] S. Moudgalya, B. A. Bernevig, and N. Regnault, Quantum many-body scars and Hilbert space fragmentation: a review of exact results, Rep. Prog. Phys. **85**, 086501 (2022).

[46] M. Serbyn, D. A. Abanin, and Z. Papić, Quantum many-body scars and weak breaking of ergodicity, Nat. Phys. **17**, 675 (2021).

[47] A. Geißler and J. P. Garrahan, Slow dynamics and nonergodicity of the bosonic quantum East model in the semiclassical limit, Phys. Rev. E **108**, 034207 (2023).

[48] B. Bertini, P. Kos, and T. Prosen, Localized dynamics in the Floquet quantum East model, Phys. Rev. Lett. **132**, 080401 (2024).

[49] B. Bertini, C. De Fazio, J. P. Garrahan, and K. Klobas, Exact quench dynamics of the Floquet quantum East model at the deterministic point, Phys. Rev. Lett. **132**, 120402 (2024).

[50] See Supplemental Material at http://link.aps.org/supplemental/10.1103/PhysRevB.110.L100304 for weakly entangled eigenstates, anomalous zero modes, convergence analysis, and additional information about the skewness fitting procedure.

[51] T. Antal, Z. Rácz, A. Rákos, and G. M. Schütz, Transport in the *XX* chain at zero temperature: Emergence of flat magnetization profiles, Phys. Rev. E **59**, 4912 (1999).

[52] D. Gobert, C. Kollath, U. Schollwöck, and G. Schütz, Real-time dynamics in spin-1/2 chains with adaptive time-dependent density matrix renormalization group, Phys. Rev. E **71**, 036102 (2005).

[53] H.-C. Jiang and T. P. Devereaux, Superconductivity in the doped Hubbard model and its interplay with next-nearest hopping t', Science **365**, 1424 (2019).

[54] X. Dong, L. Del Re, A. Toschi, and E. Gull, Mechanism of superconductivity in the Hubbard model at intermediate interaction strength, Proc. Natl. Acad. Sci. USA **119**, e2205048119 (2022).

[55] M. Ljubotina, M. Žnidarič, and T. Prosen, Kardar-Parisi-Zhang physics in the quantum Heisenberg magnet, Phys. Rev. Lett. **122**, 210602 (2019).

[56] G. Vidal, Efficient classical simulation of slightly entangled quantum computations, Phys. Rev. Lett. **91**, 147902 (2003).

[57] Note that the LDW state is an eigenstate of $\hat{n}_i(0)$, thus computing the expectation value of $\hat{n}_j(t)$ gives us direct access to the correlation function $\hat{n}_i(0)\hat{n}_j(t)$ evaluated in the LDW state. See Supplemental Material [50] for further details.

[58] B. Sutherland, *Beautiful Models: 70 Years of Exactly Solved Quantum Many-Body Problems* (World Scientific, Singapore, 2004).

[59] E. Ilievski, J. De Nardis, S. Gopalakrishnan, R. Vasseur, and B. Ware, Superuniversality of superdiffusion, Phys. Rev. X **11**, 031023 (2021).

[60] M. Žnidarič, Spin transport in a one-dimensional anisotropic Heisenberg model, Phys. Rev. Lett. **106**, 220601 (2011).

[61] M. Ljubotina, M. Žnidarič, and T. Prosen, Spin diffusion from an inhomogeneous quench in an integrable system, Nat. Commun. **8**, 16117 (2017).

[62] E. Ilievski, J. De Nardis, M. Medenjak, and T. Prosen, Superdiffusion in one-dimensional quantum lattice models, Phys. Rev. Lett. **121**, 230602 (2018).

[63] T. Iadecola and M. Žnidarič, Exact localized and ballistic eigenstates in disordered chaotic spin ladders and the Fermi-Hubbard model, Phys. Rev. Lett. **123**, 036403 (2019).

[64] C. Hess, C. Baumann, U. Ammerahl, B. Büchner, F. Heidrich-Meisner, W. Brenig, and A. Revcolevschi, Magnon heat transport in $(Sr, Ca, La)_{14}Cu_{24}O_{41}$, Phys. Rev. B **64**, 184305 (2001).

[65] A. V. Sologubenko, T. Lorenz, H. R. Ott, and A. Freimuth, Thermal conductivity via magnetic excitations in spin-chain materials, J. Low Temp. Phys. **147**, 387 (2007).

[66] J. Simon, W. S. Bakr, R. Ma, M. E. Tai, P. M. Preiss, and M. Greiner, Quantum simulation of antiferromagnetic spin chains in an optical lattice, Nature (London) **472**, 307 (2011).

[67] N. Shiraishi and T. Mori, Systematic construction of counterexamples to the eigenstate thermalization hypothesis, Phys. Rev. Lett. **119**, 030601 (2017).

[68] M. Fishman, S. R. White, and E. M. Stoudenmire, The ITensor software library for tensor network calculations, SciPost Phys. Codebases, 4 (2022).